

Evolution of Fishtail-effect with aging in pure and Ag-doped MG-YBCO

D. A. Lotnyk,* R. V. Vovk, M. A. Obolenskii, and A. A. Zavgorodniy

Physical department, V.N. Karazin Kharkov National University, 4 Svoboda Square, 61077 Kharkov, Ukraine.

J. Kováč, M. Kaňuchová, M. Šefčíková, V. Antal, and P. Diko

*Material Physics Laboratory, Institute of Experimental Physics,
Slovak Academy of Sciences, Watsonova 47, 04001 Košice, Slovakia*

A. Feher

Centre of Low Temperature Physics, P.J. Šafarik University, Park Angelinum 9, 041 54 Košice, Slovakia

(Dated: February 19, 2009)

$M(B)$ -curves were experimentally investigated. Fishtail-effect (FE) was observed in MG $\text{YBa}_2\text{Cu}_3\text{O}_{7-\delta}$ and $\text{YBa}_2\text{Cu}_{3-x}\text{Ag}_x\text{O}_{7-\delta}$ (at $x \approx 0.02$) crystals in a wide temperature range $40 \text{ K} < T < 75 \text{ K}$ at the orientation of magnetic field $\mathbf{H} \parallel c$. It was obtained that the influence of bulk pinning on FE is more effective at low temperatures while the influence of surface barriers is more effective at high temperatures. The value H_{max} for Ag-doped crystals is larger than for a pure one that due to the presence of additional pinning centers, above all on silver atoms.

PACS numbers: 74.25.Qt, 74.72.Bk, 74.81.Bd

I. INTRODUCTION

Since the discovery of high-temperature superconductors (HTSCs), their engineering applications at liquid nitrogen temperatures have drawn much attention. The $\text{YBa}_2\text{Cu}_3\text{O}_{7-\delta}$ (YBCO) is one of the promising HTSCs materials for various technical applications. However, in ceramic materials the critical current density (J_c) is, due to the weak link effects, very low, rendering them unsuitable for applications. In order to enhance J_c , the so-called melt-textured growth (MG) process [1] has been developed, which can significantly enhance J_c . One interesting phenomenon in the MG HTSCs is the fishtail effect (FE) in J_c as well as in isothermal magnetic hysteresis loops ($M(H)$ curves) [2, 3, 4]. As for the FE origin, some researchers propose the vortex ordered phase to disordered phase transition [5, 6, 7] to explain this interesting phenomenon, while others attribute it to the bulk pinning [2, 3, 4]. In the vortex phase transition explanation, the FE exists both on a single $J_c(T)$ curve and on a single $J_c(H)$ curve. However, in the bulk pinning explanation, the FE appears on $M(H)$ curves whereas on a single magnetization vs. temperature $M(T)$ curve it is seldom reported. In the previous work, the critical state model is used to study the isothermal $M(H)$ curves [8]. However, for HTSCs, due to their operation at higher temperatures and due to their small activation energy U , the flux creep is significant. Hence, non-linear flux creep models were developed. Meanwhile, the surface barrier [9], which prevents vortex entering (H_{en}) and exiting (H_{ex}) superconductors, has strong effects on the irreversibility of HTSCs. The goal of this work was to contribute to the understanding of the FE origin in terms

of significant influence of both bulk pinning and surface barriers.

II. EXPERIMENT DETAILS AND SAMPLES

MG samples $\text{YBa}_2\text{Cu}_3\text{O}_{7-\delta}$ and $\text{YBa}_2\text{Cu}_{3-x}\text{Ag}_x\text{O}_{7-\delta}$ were grown as was described in [10]. Two samples, pure crystal (S1) and Ag-doped crystal (S2), were used in the present work. Physical properties of the samples are presented in Table I. The measurements of isother-

Sample	T_c , K	ΔT_c , K	$a(b) \times b(a) \times c$, mm ³	m , mg
S1	90.2-89.8	1.0	$2 \times 1.8 \times 0.7$	12.2
S2	91.3-91.1	1.5	$1.7 \times 1.6 \times 0.8$	17.98

TABLE I: Physical characteristics for samples $\text{YBa}_2\text{Cu}_3\text{O}_{7-\delta}$ (S1) and $\text{YBa}_2\text{Cu}_{3-x}\text{Ag}_x\text{O}_{7-\delta}$ (S2)

mal hysteresis loops ($M(H)$ curves) at various temperatures ($20 \text{ K} < T < 85 \text{ K}$) were carried out in fields ($-6 \text{ T} < H < 6 \text{ T}$) parallel to the c -axis by means of a commercial vibrating sample magnetometer (VSM). The field sweep rate was $dH/dt \approx 0.1 \text{ T/min}$. To obtain an additional parameter ΔT_c the resistivity $R(T)$ curves were measured on two samples (the first one is pure and the second one is Ag-doped) which were obtained from the same single-domain bulks as S1 and S2. Transport measurements were performed using a physical property measurement system (PPMS). The experiment was divided into two steps. $M(H)$ curves were measured: a) right after annealing of samples in oxygen (during 240 hours at 400°C); b) after long-term aging at the room temperature (six months), in which case almost all relaxation processes were finished. The first value for T_c in Table I corresponds to a) and the second value corresponds to b).

*Electronic address: dmitry.a.lotnik@univer.kharkov.ua

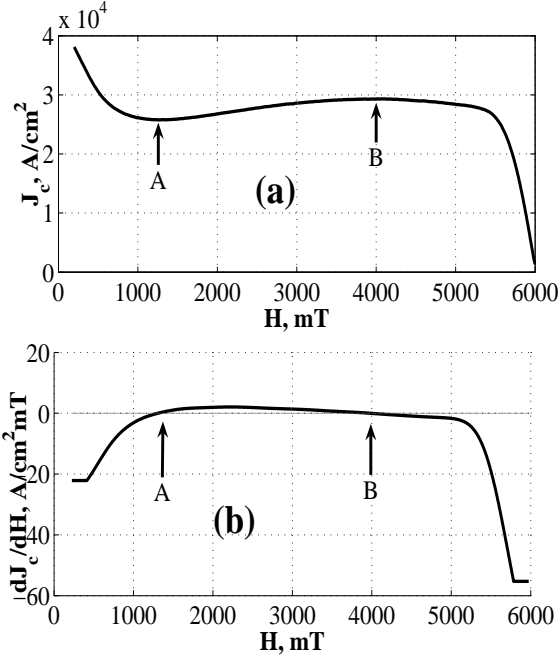


FIG. 1: Field dependences of critical current density J_c (a) and derivative dJ_c/dH (b) at temperature $T=70$ K for sample S1 right after annealing. Points A and B denotes positions of minimum and maximum respectively.

III. MODEL TO ANALYZE EXPERIMENTAL DATA

From the measured $M(H)$ curves the critical current density was calculated using the critical state model [11] that have been developed in [12]:

$$J_c = 2\Delta M \frac{\rho}{a^2(b - a/3)c}, \quad (1)$$

where $\Delta M = M_1(H) - M_2(H)$ ($M_1(H) > 0$, $M_2(H) < 0$) are the values of magnetic moment at field H , ρ is the density of sample, a, b and c are geometric dimensions of sample. Dependences $J_c(H)$ (Fig. 1a for $T=70$ K) were calculated for the field range $0 < H < 6$ T. To obtain the exact position of maximum on $J_c(H)$ curves the derivative dJ_c/dH was calculated for each temperature (see example at Fig. 1b). Fig. 1 shows positions of both minimum (point A) and maximum (point B) on J vs H curve, where derivative $dJ_c/dH = 0$. Then the 3D surface $T - H - dJ_c/dH$ was obtained. Intermediate curves were defined by the 3rd degree polynomial (spline-function). The contour for $dJ_c/dH = 0$ is shown in Fig. 2. Points A and B correspond to those in Fig. 1. This method is useful to obtain position of maximum $J_{c,max}$ (or ensemble of points B) not only at given temperatures but also for intermediate temperatures.

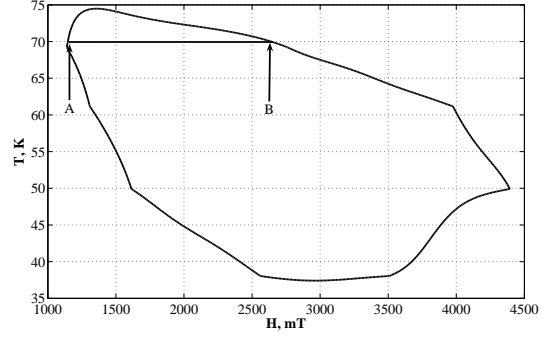


FIG. 2: Contour for $dJ_c/dH = 0$ for sample S1 right after annealing. Points A and B coincide with points A and B in the Fig. 1

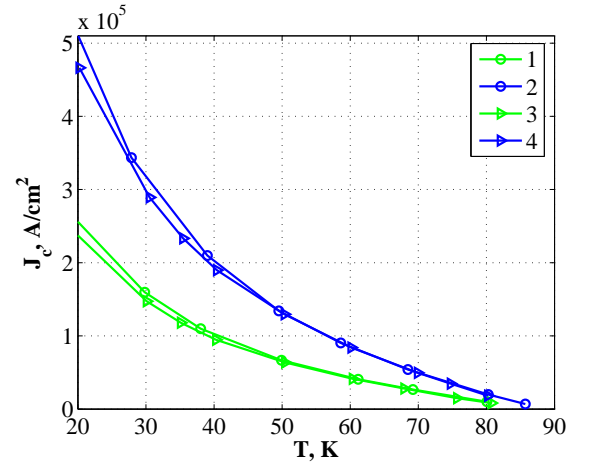


FIG. 3: Temperature dependences of critical current density at zero magnetic field for samples S1 (green lines) and S2 (blue lines), right after annealing (curves 1,2) and after long-term aging (curves 3,4)

IV. RESULTS AND DISCUSSIONS

Fig. 3 shows the temperature dependences $J_c(T)$, on which FE appears. However, according to [5, 6, 7], FE appears not due to the order-disorder phase transition of vortex lattice. The possible reason of the FE existence is a significant influence of both bulk pinning and surface barriers [13]. From the model in previous chapter the $H - T$ dependences of $J_{c,max}$ were obtained (see Fig. 4). As one can see from Table I the value of the critical temperature T_c for sample S1 changed from 90.2 K to 89.8 K and for sample S2 changed from 91.3 K to 91.1 K. This indicates the optimal oxygen annealing process and aging effects are not caused by changing in δ (especially for sample S2). According to the estimations performed in [13] the surface barriers are more important at high temperatures while the bulk pinning is more important at low temperatures. As one can see from Fig. 4 the position of $J_{c,max}$ significantly evolves after

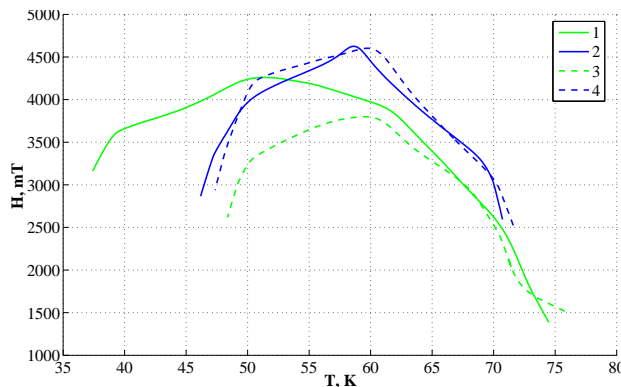


FIG. 4: Temperature-field dependences of $J_{c,max}$ -position for samples S1 (green lines) and S2 (blue lines), right after annealing (curves 1,2) and after long-term aging (curves 3,4)

long-term aging. The maximum field H_{max} for sample S1 decreases from 4.25 T to 3.8 T and the minimum temperature T_{min} increases from 37.5 K to 48 K (curves 1 and 3 in Fig. 4). Such changes can be induced by the redistribution of pinning centers in the crystal or, in another words, bulk pinning changes during aging. Constancy of the maximum temperature T_{max} for S1 corresponds to the influence of surface barriers at high temperatures. The aging effect for sample S2 is not so significant as for S1. It is related to the presence of considerable mechanical tensions in the sample (large value of an additional parameter $\Delta T_c = 1.5$ K) that prevent the redistribution of pinning centers. Larger value of H_{max} (for S2 as compared with S1) corresponds to the presence of additional pinning centers on silver atoms [14].

A possible reason of the decrease of H_{max} and increase of T_{min} for S1 is the decreasing number of dislocations. In another words, the crystal S1 becomes more homogeneous after aging.

V. CONCLUSIONS

In summary, MG YBCO samples were investigated by measuring $M(B)$ -curves. On these curves FE was observed in a wide temperature range. The origin of the FE existence is a significant influence of both surface barrier and bulk pinning. Bulk pinning influences parameters H_{max} and T_{min} while surface barrier influences T_{max} . Undoped YBCO is characterized by a significant aging effect which is manifested in a considerable change of H_{max} and T_{min} . This corresponds to the change of bulk pinning. For Ag-doped YBCO there are no significant changes in H_{max} , T_{min} and T_{max} . Such difference is caused by the redistribution of pinning centers in undoped YBCO while Ag-doped YBCO is characterized by huge mechanical tensions which prevent redistribution. Possible origin of redistribution for S1 is a decrease in number of dislocations, i.e. sample becomes more homogenous.

Acknowledgments

The work was partly supported by the Slovak Research and Development Agency (No. APVV-0006-07) and the Slovak Grant Agency VEGA (No.1/0159/09) The financial support of U.S.Steel - DZ Energetika Košice is acknowledged. One of author (D.L.) is very thankful to the National Scholarship Program of Slovak Republic (SAIA) for the financial support during his stay in Slovakia.

-
- [1] S. Jin, T. H. Tiefel, R. C. Sherwood, M. E. Davis, R. B. van Dover, G. W. Kammiott, R. A. Fastnache and H. D. Keith, *Appl. Phys. Lett.* **52**, 2074 (1988).
 - [2] M. Muralidhar, N. Sakai, N. Chikumoto, M. Jirsa, T. Machi, M. Nishiyama, Y. Wu and M. Murakami, *Phys. Rev. Lett.* **89**, 237001 (2002).
 - [3] M. R. Koblishka and M. Murakami, *Supercond. Sci. Technol.* **13**, 738 (2000).
 - [4] M. Muralidhar, M. Jirsa, M. Sakai and M. Murakami, *Supercond. Sci. Technol.* **16**, R1 (2003).
 - [5] W. Henderson, E. Y. Andrei, M. J. Higgins and S. Bhattacharya, *Phys. Rev. Lett.* **77**, 2077 (1996).
 - [6] Y. Paltiel, E. Zeldov, Y. N. Myasoedov, H. Shtrikman, S. Bhattacharya, M. J. Higgins, Z. L. Xiao, E. Y. Andrei, P. L. Gammel and D. J. Bishop, *Nature* **403**, 398 (2000).
 - [7] Y. Paltiel, E. Zeldov, Y. N. Myasoedov, M. L. Rappaport, G. Jung, S. Bhattacharya, M. J. Higgins, Z. L. Xiao, E. Y. Andrei, P. L. Gammel, et al., *Phys. Rev. Lett.* **85**, 3712 (2000).
 - [8] T. H. Johansen, M. R. Koblishka, H. Bratsberg and P. O. Hetland, *Phys. Rev. B* **56**, 11273 (1997).
 - [9] C. P. Bean and J. D. Livingston, *Phys. Rev. Lett.* **12**, 14 (1964).
 - [10] P. Diko, M. Šefciková, M. Kaňuchová and K. Zmorayová, *Materials Science and Engineering B* **151**, 7 (2008).
 - [11] C. P. Bean, *Phys. Rev. Lett.* **8**, 14 (1962).
 - [12] H. P. Wiesinger, F. M. Sauerzopf and H. W. Weber, *Physica C* **203**, 121 (1992).
 - [13] L. Zhang, Q. Qiao, X. B. Xu, Y. L. Jiao, L. Xiao, S. Y. Ding and X. L. Wang, *Physica C* **445-448**, 236 (2006).
 - [14] T. Nakashima, Y. Ishii, T. Katayama, H. Ogino, S. Horii, J. Shimoyama and K. Kishio, *J. Phys.: Conf. Ser.* **97**, 012007 (2008).